

# Persistence of Birefringence in Sheared Solutions of Wormlike Micelles

Bradley D. Frounfelker,<sup>†,§</sup> Gokul C. Kalur,<sup>†,||</sup> Bani H. Cipriano,<sup>†,⊥</sup> Dganit Danino,<sup>‡</sup> and Srinivasa R. Raghavan<sup>\*,†</sup>

Department of Chemical & Biomolecular Engineering, University of Maryland, College Park, Maryland 20742-2111, and Department of Biotechnology and Food Engineering, Technion - Israel Institute of Technology, Technion, Haifa, Israel 32000

Received September 6, 2008. Revised Manuscript Received October 27, 2008

When aqueous solutions containing wormlike micelles (worms) are sheared, the micellar chains tend to align with the flow, which in turn leads to flow-birefringence. When shear is stopped, the worms rapidly revert to an isotropic state in typical samples, and the birefringence disappears. In this study, we present a system of cationic worms that shows a different behavior: not only do the samples become intensely birefringent when sheared but the *birefringence also persists for hours* (and even days) after shear is stopped. These results suggest that shear-aligned worms in the sample are trapped in their aligned state for long periods of time, an aspect that is confirmed by cryo-transmission electron microscopy (cryo-TEM). We seek to determine the origin of this unusual behavior. Our results show that the persistent birefringence is observed for cationic worms induced by *hydroxy-naphthoate* but not salicylate counterions. These observations suggest that the micellar alignment is stabilized by intermicellar attractive interactions (such as  $\pi$ - $\pi$  and cation- $\pi$ ) that arise when large aromatic counterions are anchored within the micelles.

## 1. Introduction

The term “wormlike micelles” refers to long and flexible micellar chains having a cylindrical cross section.<sup>1–4</sup> Such micelles (“worms” for short) are formed in aqueous solution by the self-assembly of surfactant molecules. For example, worms can be formed by the combination of a long-tailed cationic surfactant (such as cetyl trimethylammonium bromide, CTAB) with an inorganic salt (such as NaCl) or an organic salt (such as sodium salicylate, NaSal).<sup>1–4</sup> The salt is necessary to mitigate the electrostatic repulsions between the cationic headgroups of the surfactant and thereby promote the association of surfactant molecules into long, wormlike chains. Cationic worms such as the above find use in industrial applications such as hydraulic fracturing for tertiary oil recovery.<sup>3</sup>

The presence of worms can be indirectly inferred from two characteristic features of the sample: its pronounced viscoelasticity and its flow-birefringence.<sup>1–4</sup> The viscoelasticity arises because worms entangle with each other, much like polymer chains. Flow-birefringence is the property by which the sample shows birefringence when sheared.<sup>5–7</sup> For example, when a vial containing the sample is shaken, intense streaks of light are observed in the sample as it is viewed under crossed polarizers (Figure 1a; also see Movie 1a in the Supporting Information). The microstructural origin of flow-birefringence is that, when an isotropic entangled network of worms is sheared, segments of the worms disentangle and align with the flow direction.<sup>5</sup> Domains

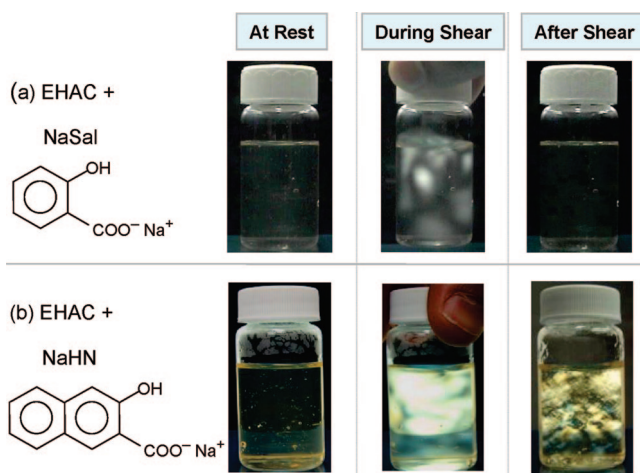


**Figure 1.** Photographs of two wormlike micellar solutions under crossed polarizers. The sample in (a) is a mixture of 40 mM EHAC + 300 mM NaSal, while that in (b) contains 40 mM EHAC + 160 mM NaHN. At rest, both samples are isotropic and hence appear dark. When the vials are shaken vigorously, both samples exhibit streaks of light (flow-birefringence). When the shearing is stopped, sample (a) reverts rapidly to its initial isotropic state. On the other hand, sample (b) remains strongly birefringent even days later. Movies accompanying these images are provided in the Supporting Information.

of aligned worms exhibit differences in their refractive index along mutually perpendicular directions, which manifests as birefringence.

Given the above typical behavior of worms, one might ask what would happen to the worms when shear is stopped. Specifically, this question can be directed to both the rheology and the flow-birefringence. Considering the rheology first, the application of shear is known to cause disentanglement of worms, leading to a drastic reduction in viscoelastic properties (e.g., shear-thinning in steady-shear). How long will it then take for the sample to “reheal”, that is, for its original (at-rest) rheological properties to be restored? Second, with regard to the flow-birefringence, does the birefringence persist once shear is

\* To whom correspondence should be addressed. E-mail: sraghava@eng.umd.edu.

<sup>†</sup> University of Maryland.

<sup>‡</sup> Technion - Israel Institute of Technology.

<sup>§</sup> Present address: Army Research Laboratory, Aberdeen Proving Ground, MD.

<sup>||</sup> Present address: Irix Pharmaceuticals Inc., Florence, SC.

<sup>⊥</sup> Present address: Balchem Inc., New Hampton, NY.

(1) Cates, M. E.; Candau, S. J. *J. Phys.: Condens. Matter* **1990**, *2*, 6869.

(2) Rehage, H.; Hoffmann, H. *Mol. Phys.* **1991**, *74*, 933.

(3) Ezrahi, S.; Tuval, E.; Aserin, A. *Adv. Colloid Interface Sci.* **2006**, *128*, 77.

(4) Dreiss, C. A. *Soft Matter* **2007**, *3*, 956.

(5) Larson, R. G. *The Structure and Rheology of Complex Fluids*; Oxford University Press: Oxford, 1999.

(6) Shikata, T.; Dahman, S. J.; Pearson, D. S. *Langmuir* **1994**, *10*, 3470.

(7) Schubert, B. A.; Kaler, E. W.; Wagner, N. J. *Langmuir* **2003**, *19*, 4079.

stopped, or does the sample revert to its isotropic state very quickly? With regard to the latter, typical worm samples show the response depicted in Figure 1a (also see Movie 1a, Supporting Information). Initially, the sample is not birefringent, indicating that the entangled worm network is isotropic. When sheared, the sample shows birefringence, but as soon as shear is stopped, the birefringence vanishes. This can be also seen in typical rheo-optic data, for example, in the paper by Kaler et al.<sup>7</sup> Indeed, this is why the phenomenon is termed *flow-birefringence*—to indicate that the birefringence appears only during flow.

In this paper, we describe a series of worms that show a very different behavior with regard to birefringence. This is indicated in Figure 1b; see also Movie 1b in the Supporting Information. The samples consist of a well-known cationic surfactant, erucyl bis(hydroxyethyl)methyl ammonium chloride (EHAC)<sup>8</sup> and a naphthalene derivative (sodium hydroxynaphthoate, NaHN).<sup>9,10</sup> Figure 1b shows that the EHAC/NaHN sample is initially isotropic, much like the control sample in Figure 1a. When the vial is shaken, the sample becomes intensely birefringent. When shear is stopped, the birefringence decreases a bit, *but the sample remains strongly birefringent at rest*. In fact, the sample persists in this birefringent state for several hours and, in many cases, even for several days.

Intrigued by the above visual observations, we have studied EHAC/NaHN worms in more detail. For comparison, we also study worms formed by the same surfactant, i.e., EHAC, with the oft-used organic counterion, NaSal (the control sample in Figure 1a is an EHAC/NaSal solution).<sup>8</sup> Structurally, NaSal and NaHN are similar, except that the latter has an extra benzene ring (structures shown in Figure 1). The interesting finding from our study is that birefringence persists long after shear is stopped only for EHAC/NaHN samples and not for EHAC/NaSal ones. Even within the EHAC/NaHN system, the phenomenon is restricted to certain sample compositions. What is the molecular or structural origin for the persistent birefringence? Why does this occur only with certain wormlike micellar systems? These are some of the questions addressed in this paper. We use rheological studies, flow-birefringence measurements (both qualitative and quantitative), measurements of small-angle neutron scattering under flow (flow-SANS), and cryo-transmission electron microscopy (cryo-TEM) to investigate our samples.

## 2. Experimental Section

**Materials and Sample Preparation.** The cationic surfactant EHAC has a molecular formula  $C_{22}H_{43}-N^+(CH_2OH)_2-CH_3Cl^-$  with a *cis* double bond between the 9th and 10th carbon atoms in the tail. It was a commercial product from Akzo Nobel, Chicago, IL. Details on this material as well as on EHAC-based worms have been reported in our previous studies<sup>8,11–13</sup> and by others.<sup>14–17</sup> NaSal and NaHN were obtained from Sigma; the structures of these salts are shown in Figure 1a and b, respectively. Solutions containing surfactant and

salt were prepared using distilled–deionized water. Samples were stored under ambient conditions and were stable for more than 1 year.

**Rheology.** Rheological experiments were conducted at 25 °C on a Rheometrics RDA-III strain-controlled rheometer using parallel-plate and cone-plate geometries, both of which were equipped with Peltier-based temperature control. Dynamic frequency sweeps were conducted within the linear viscoelastic regime of the samples, as determined previously from strain-sweep experiments. Sample reheal after shear was also studied; these experiments are described in the Results and Discussion section.

**Flow-Birefringence.** Rheo-optic experiments were performed using the Optical Analysis Module (OAM) mounted on a Rheometrics DSR rheometer. The sample was placed between parallel plates of diameter 25 mm, with a gap of 1 mm. Linearly polarized light from a He–Ne laser ( $\lambda = 632.8$  nm) was passed through the sample parallel to the axis of rotation, thereby enabling rheo-optic studies in the flow-vorticity plane. Analysis of the transmitted light yielded the flow-birefringence ( $\Delta n'$ ).

**Flow Small-Angle Neutron Scattering (Flow-SANS).** Flow-SANS experiments were conducted on the NG-3 (30 m) beamline at NIST, Gaithersburg, MD. The sample was placed in a quartz Couette cell with an outer rotating cylinder of radius 29.5 mm and an annulus of 0.5 mm. Experiments were conducted at 25 °C in the radial direction, with the beam perpendicular to the Couette axis, which yields the two-dimensional scattering pattern in the flow-vorticity plane. The intensity  $I$  as a function of the wave vector  $q$  can be obtained by a radial average of the 2-D pattern, and this can be placed on an absolute scale using calibration standards provided by NIST.

**Optical Microscopy.** Samples were examined using an Olympus microscope in crossed polarizer mode and using objectives of 2.5× and 10× magnification.

**Cryo-TEM.** Samples for cryo-TEM were prepared using a controlled environment vitrification system (CEVS).<sup>18</sup> The procedure involved spreading the sample on a TEM grid using blotting paper (this process involved high shear), followed by rapid quenching of the grid into liquid ethane (−183 °C) to form a vitrified specimen. The sample was thereafter examined on a Philips CM120 microscope (120 kV), with an Oxford CT-3500 cryo-holder maintaining the sample temperature below −180 °C. Digital images were recorded by using a Gatan 791 MultiScan CCD camera in the minimal electron dose mode.<sup>18</sup>

## 3. Results and Discussion

First, it is useful to place the rheological data in the context of the phase behavior of the system. The phase behavior of 40 mM EHAC solutions as a function of NaHN concentration and temperature has been reported earlier<sup>13</sup> and is replotted in Figure 2. At 25 °C, as the NaHN concentration ( $c_{\text{NaHN}}$ ) is increased, one finds a two-phase region from about 20 to 70 mM NaHN. Our interest in this paper is in samples to the right of this region, that is, from about 75 to 250 mM NaHN. Over this range, the samples are viscoelastic, one-phase solutions at 25 °C. As an aside, all these samples show cloud-point behavior;<sup>13</sup> that is, they phase-separate when heated above the cloud point curve, shown in red. This phenomenon has been discussed previously;<sup>13</sup> it is not important here.

The focus of this paper is on the rheology and flow-birefringence along the 25 °C line as a function of  $c_{\text{NaHN}}$ . Figure 3 shows the zero-shear viscosities  $\eta_0$  of samples containing 40 mM EHAC and 80–240 mM NaHN. As  $c_{\text{NaHN}}$  is increased,  $\eta_0$  increases to a maximum and then decreases. Samples near the viscosity maximum were extremely viscoelastic and almost gel-like. It was these same samples that showed the persistent flow-induced birefringence. For reference, the region of persistent

(8) Raghavan, S. R.; Kaler, E. W. *Langmuir* **2001**, *17*, 300.

(9) Mishra, B. K.; Samant, S. D.; Pradhan, P.; Mishra, S. B.; Manohar, C. *Langmuir* **1993**, *9*, 894.

(10) Horbaschek, K.; Hoffmann, H.; Thunig, C. J. *Colloid Interface Sci.* **1998**, *206*, 439.

(11) Raghavan, S. R.; Edlund, H.; Kaler, E. W. *Langmuir* **2002**, *18*, 1056.

(12) Schubert, B. A.; Wagner, N. J.; Kaler, E. W.; Raghavan, S. R. *Langmuir* **2004**, *20*, 3564.

(13) Kalur, G. C.; Frounfelker, B. D.; Cipriano, B. H.; Norman, A. I.; Raghavan, S. R. *Langmuir* **2005**, *21*, 10998.

(14) Couillet, I.; Hughes, T.; Maitland, G.; Candau, F.; Candau, S. J. *Langmuir* **2004**, *20*, 9541.

(15) Siriawatwechakul, W.; Lafleur, T.; Prud'homme, R. K.; Sullivan, P. *Langmuir* **2004**, *20*, 8970.

(16) Croce, V.; Cosgrove, T.; Maitland, G.; Hughes, T.; Karlsson, G. *Langmuir* **2003**, *19*, 8536.

(17) Croce, V.; Cosgrove, T.; Dreiss, C. A.; King, S.; Maitland, G.; Hughes, T. *Langmuir* **2005**, *21*, 6762.

(18) Danino, D.; Bernheim-Groswasser, A.; Talmon, Y. *Colloids Surf., A* **2001**, *183*, 113.

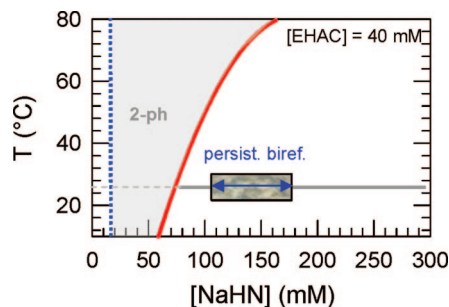


**Figure 2.** Phase behavior of 40 mM EHAC + NaHN solutions as a function of the NaHN concentration (replotted from ref 13). The persistent birefringence was mainly studied for samples at room temperature (25 °C), indicated by the solid line. The phenomenon was particularly striking for samples over the concentration range shown by the window.

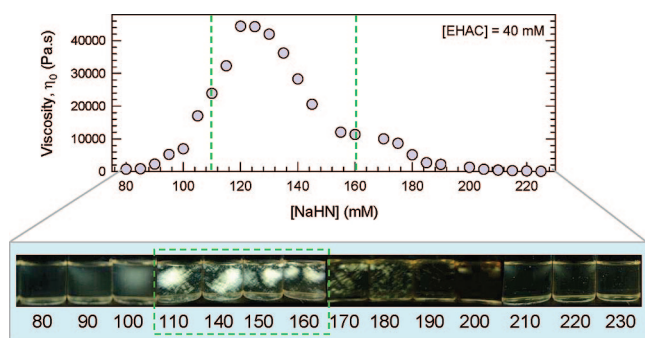


**Figure 3.** Zero-shear viscosity  $\eta_0$  of 40 mM EHAC solutions as a function of the NaHN concentration. The bottom panel compares the birefringence of these solutions following a controlled amount of shear (see text for details). Numbers below the images in the panel correspond to NaHN concentrations. Note that the pronounced birefringence is seen for NaHN concentrations around the viscosity maximum (marked by dashed lines).

birefringence is also marked on the phase diagram (Figure 2): it occurs over a relatively narrow range of  $c_{\text{NaHN}}$  just to the right of the two-phase region.

The intense, persistent birefringence in certain EHAC/NaHN samples could be observed visually. Even just tapping or lightly shaking the vials of these samples gave rise to pronounced birefringence,<sup>9,10</sup> as shown in Figure 1b (and Movie 1b, Supporting Information). For some viscoelastic samples ( $<100$  mM or  $>190$  mM NaHN), the birefringence decayed within a few minutes, once shear was stopped (regardless of the intensity of the shear). However, for  $c_{\text{NaHN}}$  from 110 to 160 mM, the birefringence remained intense long after shear was stopped. To compare the residual birefringence in a systematic manner, the following procedure was used. Sample vials corresponding to different  $c_{\text{NaHN}}$  were loaded into a centrifuge and spun at 1000 rpm for 10 min. The samples were then unloaded from the centrifuge and photographed side by side (through crossed polarizers). Such a photograph is shown in the bottom panel of Figure 3. Note the distinctive birefringent appearance of samples between 110 and 160 mM NaHN; from the viscosity data, these are samples spanning the viscosity maximum.

The birefringence of sheared EHAC/NaHN samples can also be observed under an optical microscope equipped with crossed polarizers. Typical micrographs are shown in Figure S1 in the Supporting Information; the data are for a 40 mM EHAC + 110 mM NaHN sample that had been previously subjected to shear in the centrifuge. Both micrographs show birefringent domains and defects characteristic of aligned phases.<sup>5</sup> Similar birefringence could be seen in all samples within the 110–160 mM NaHN

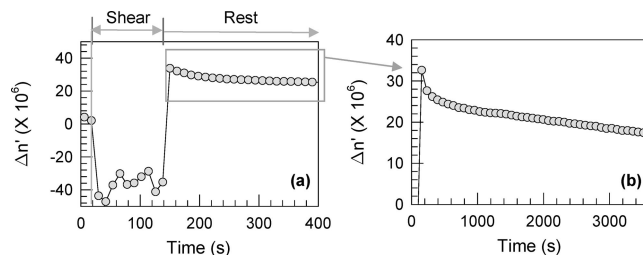


**Figure 4.** (a) Birefringence ( $\Delta n'$ ) during and after shear for a 40 mM EHAC + 110 mM NaHN sample. Initially, at rest, the sample is isotropic ( $\Delta n' = 0$ ). When steady-shear at  $5 \text{ s}^{-1}$  is applied,  $\Delta n'$  becomes strongly negative. When the shear is stopped,  $\Delta n'$  switches sign but remains significant in magnitude, decaying very slowly. The slow decay is evident in (b), where the time axis is extended to 1 h.

range. We also conducted a few experiments at higher EHAC concentrations. The higher the EHAC concentration (i.e., the higher the volume fraction of worms), the stronger was the observed birefringence (data not shown). This was evident both from visual observations of sample vials as well as by optical microscopy.

While the above observations are qualitative, we have also done a limited number of quantitative rheo-optic studies on EHAC/NaHN samples to quantify their birefringent properties. Figure 4 shows the birefringence  $\Delta n'$  during and after shear for the 40 mM EHAC + 110 mM NaHN sample. When sheared at  $5 \text{ s}^{-1}$  (Figure 4a), the sample exhibited a strongly negative  $\Delta n'$  (the data are erratic, presumably due to shear-banding of worms at this shear rate). As soon as shear is stopped,  $\Delta n'$  flips sign from negative to positive, but the magnitude of the birefringence remains high even hours afterward (Figure 4b extends the time axis to about 1 h). The flipping of the  $\Delta n'$  sign is not understood, and it did not occur in all experiments. Nevertheless, the basic result tallies with the visual and optical findings, which is that the birefringence decays very slowly after shear is stopped. Fitting the data in Figure 4b to an exponential decay gives a decay time of about 6 h. Further rheo-optic experiments over a range of shear-rates were not done because of the difficulties in working with these highly viscous fluids: the glass plates used for these experiments were smooth surfaces, which gave rise to considerable wall-slip.

Our focus in this study is on elucidating *why* the birefringence persists in certain worm samples. Also, how should one interpret this phenomenon: is it a shear-induced phase transition, or is it a nonequilibrium, kinetically trapped state driven by shear? All the evidence points to it being a nonequilibrium effect. As mentioned, the birefringence does decay away, albeit slowly, when the sample is stored under ambient conditions. In this context, the decay of the birefringence can be accelerated by increasing the temperature. This is illustrated by Figure 5. Here, the sample (40 mM EHAC + 110 mM NaHN) is placed in a water bath at 50 °C and observed under crossed polarizers. The sample is intensely birefringent at  $t = 0$ . Within minutes, however, there is an appreciable lowering of the birefringence, and in about 20 min the birefringence has completely disappeared (i.e., the sample has become isotropic). Note that there is no critical temperature above which the sample has to be heated for its birefringence to vanish. Figure 5 underscores the fact that the birefringent state is a trapped, nonequilibrium condition of the sample. Shear does not induce a phase transition from worms to a lamellar or other liquid crystalline phase; this point is also consistent with the rheology, SANS, and cryo-TEM data below.

Next, we use dynamic rheology to compare the rheological response of isotropic and birefringent worms. The following



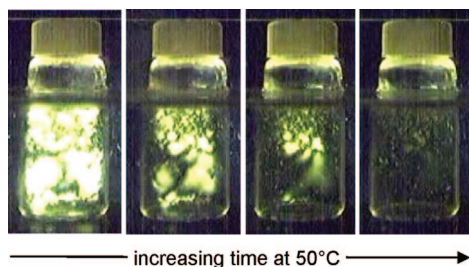


**Figure 5.** Decay of birefringence in a 40 mM EHAC + 110 mM NaHN sample upon heating. The birefringent sample is placed in a 50 °C water bath at  $t = 0$ , and the sample is observed through crossed polarizers. Photographs at 5 min intervals of time are shown.

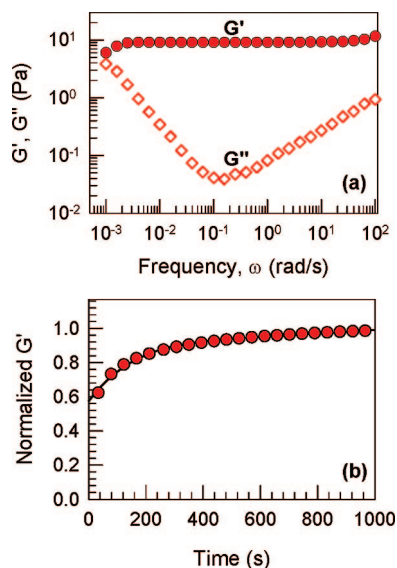


**Figure 6.** (a) Dynamic rheology of a 40 mM EHAC + 110 mM NaHN sample. The elastic modulus  $G'$  and the viscous moduli  $G''$  are shown as functions of frequency. (b) Reheal of rheological properties of the above sample following steady preshear at  $5 \text{ s}^{-1}$ . The shear is stopped at time zero and the moduli are monitored versus time at a frequency of 10 rad/s. Data are shown for  $G'$ , the value of which is normalized based on its plateau value in (a). The line through the data is a fit to a stretched exponential function.

procedure was adopted. First, the sample (same composition as above) was loaded into the rheometer, and then the temperature was raised to ensure that it became isotropic (and to erase any birefringence induced by the shear during loading). After cooling back to 25 °C, a frequency sweep was conducted, and the corresponding data for the elastic and viscous moduli,  $G'$  and  $G''$ , versus frequency  $\omega$  are shown in Figure 6a. Then, the sample was sheared at  $5 \text{ s}^{-1}$  for 5 min whereby birefringence was induced in the sample. As soon as the shear was stopped, the reheal of the viscoelastic moduli was measured as a function of time at a constant frequency of 10 rad/s (Figure 6b). Finally, a second frequency sweep was conducted to compare with the original data.

Figure 6 shows that the sample rheology reheals much more rapidly than does the birefringence. First, note that the frequency response in Figure 6a is the characteristic, Maxwell fluidlike response expected for worms. The relaxation time  $t_R$  is thus the inverse of the frequency of intersection of  $G'$  and  $G''$ , that is, about 1000 s. Upon shearing, the micellar network is disrupted, leading to lower moduli. After shear, as the sample is allowed to reheal, the moduli increase back to their original values. Figure 6b plots the normalized elastic modulus  $G'$  during reheal: here,  $G'$  has been scaled by its initial value at 10 rad/s from Figure

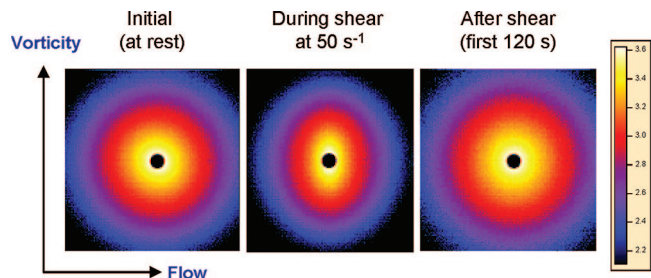


**Figure 7.** SANS patterns in the flow-vorticity plane for a 40 mM EHAC + 110 mM NaHN sample before, during, and after shear.

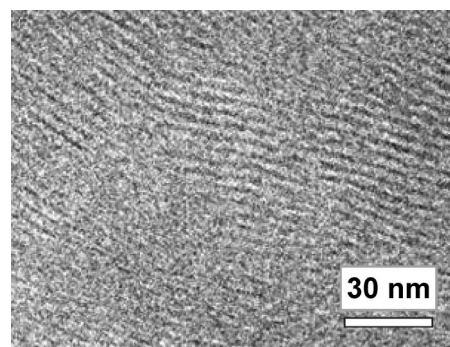


**Figure 8.** Cryo-TEM image of a 40 mM EHAC + 160 mM NaHN sample. Domains of aligned micelles are seen in the image.

6a. Note that the normalized  $G'$  reaches 1 in less than 1000 s. Fitting the reheal data in Figure 6b to a stretched exponential function gives a time constant of about 50 s, which is less than the sample's relaxation time. For comparison, recall that the time constant for the relaxation of  $\Delta n'$  from Figure 6b was about 6 h. This means the rheology is fully rehealed even though the sample is still birefringent. Also, the frequency sweep conducted after full reheal matched closely with the initial frequency data in Figure 6a. This shows that the rehealed sample (although birefringent) still exhibits a Maxwell-like response, which confirms that it still contains wormlike micelles (i.e., that there is no phase transition).

Next, we use shear-SANS to examine the structure during and after shear in the above EHAC/NaHN sample. Initially (Figure 7a), the sample shows an isotropic SANS pattern. Upon shearing at  $5 \text{ s}^{-1}$ , the pattern elongates slightly, and this is accentuated at  $50 \text{ s}^{-1}$  (Figure 7b). The elongated pattern corresponds to higher scattering intensities in the vorticity compared to the flow direction; see also the  $I$  versus  $q$  data in the Supporting Information, Figure S2. Such an elongated pattern reflects strong alignment of the micelles along the flow direction, and similar data have been reported in a number of studies.<sup>12,17,19</sup> Our interest again is in the relaxation of this pattern after shear is stopped. Generally, shear-SANS has limited time resolution,<sup>12,17,19</sup> so the data in Figure 7c correspond to the first 120 s after stopping shear. It is clear, however, that the pattern has reverted to its initial isotropic appearance, at least over the flow-vorticity plane probed in these experiments (note that micellar alignment predominantly occurs in the flow-gradient plane). Thus, shear-SANS does not detect persistent micellar alignment even though flow-birefringence is able to do so. This discrepancy can be explained in the light of the cryo-TEM images (see below). Also, circular averages of the patterns in Figure 8a and c reveal almost identical  $I(q)$  data, both of which correspond to cylindrical

micelles, meaning that there is no flow-induced transition from micelles to any other phase.

Finally, we show a typical cryo-TEM micrograph of an EHAC/NaHN sample (Figure 8). Sample preparation in cryo-TEM involves spreading a thin film on a TEM grid, which is a high-shear process.<sup>18</sup> Following spreading, the structure is allowed to relax for a few minutes before the grid is plunged into liquid ethane. If the structure does not relax in this time frame, it will be reflected in the images. One should also mention the difficulty in spreading a very thin film of samples that are highly viscous, as are the ones studied here. Because of the high sample thickness, the level of contrast in our images was low.<sup>18</sup> Nevertheless, Figure 8 is very revealing: one sees domains of aligned micellar segments, with each domain containing tens to hundreds of such segments (size scales of 50–100 nm). Note that the domains are randomly oriented with respect to each other. This may explain why the SANS pattern of such a system (Figure 7c) would be isotropic, since SANS probes the average alignment of micellar segments within all domains. On the other hand, flow-birefringence, being an optical technique, is sensitive to the alignment of entire domains, which is why we found a very slow decay of  $\Delta n'$  (Figure 5). Also, the alignment does not pervade the entire sample, so unaligned segments are presumably still entangled with each other. This would explain the rapid reheal of rheological properties (Figure 6b). It is worth mentioning that aligned worms are often seen by cryo-TEM,<sup>16,20</sup> but usually the worms are not well-correlated with respect to each other (i.e., there is no order within aligned domains). Thus, the cryo-TEM data for EHAC/NaHN samples is unusual, and it clearly correlates with the strong residual birefringence in these samples.

**Explaining the Persistent Birefringence.** Based on the cryo-TEM images, one can attribute the birefringence to aligned domains of micelles that are trapped in the sample long after shear is stopped. While the ability of worms to align under shear is well-known, the fact that their alignment can be retained after shear is indeed surprising. Generally, one would expect alignment to gradually disappear due to the randomizing effect of Brownian motion. If the worm phase is highly viscous, such Brownian motion could be slowed down, which could contribute to the trapped state of alignment. In this context, it is revealing that the strongest residual birefringence was observed for samples around the viscosity peak (Figure 3). In other words, within the EHAC/NaHN system, samples of much lower viscosity (and thereby relaxation time) did not show persistent birefringence. This partially explains why the phenomenon is localized over a certain window of NaHN concentrations.

Although sample viscosity is one factor, it is not the most important one. In particular, highly viscous worms can be formed in a variety of systems, many of which have been studied in our laboratory and by others.<sup>4,8,11,13</sup> An example is the EHAC/NaSal system:<sup>8</sup> here, over the entire range of NaSal concentrations, persistent birefringence is not observed in *any* sample (as exemplified by Figure 1a). The same is true for EHAC worms induced by other weak aromatic hydrotropes such as sodium tosylate (NaTos).<sup>11</sup> Also, EHAC worms induced by simple salts such as NaCl or KBr (i.e., inorganic counterions) do not show this effect. On the other hand, if we combine NaHN with a different cationic surfactant (CTAB, for instance, rather than EHAC), it is indeed possible to make samples with strong residual birefringence. In fact, in earlier reports of the CTAB/NaHN system by Manohar et al.<sup>9</sup> and Hoffmann et al.,<sup>10</sup> indirect references to the long-lived birefringence can be found. (We do observe that

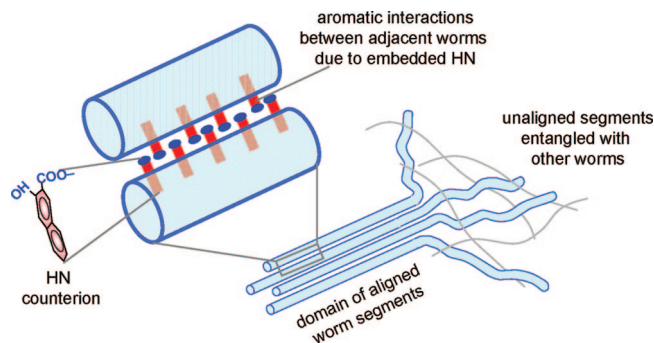


**Figure 9.** Microstructure in an EHAC/NaHN solution showing persistent birefringence. Aligned worm segments are bunched into domains, as seen in cryo-TEM. Within each domain, the alignment is preserved due to noncovalent interactions between the micellar segments. These interactions are mediated by the HN counterions embedded within the micelles and include offset-stacked  $\pi$ – $\pi$  interactions between counterions as well as cation– $\pi$  interactions between the counterions and the cationic headgroups.

the effect is even more pronounced with EHAC than with CTAB.) In sum, the nature of the surfactant is not important, but the nature of the salt (counterion) certainly is.

We believe the key requirement is the *strong hydrophobicity and aromaticity* of the counterions. Comparing NaHN and NaSal, the former has an extra benzene ring, which makes it more hydrophobic and thereby enhances its binding affinity to micelles.<sup>21,22</sup> As shown by Figure 9, the hydroxy-naphthoate (HN) counterion will insert its naphthalene ring into the hydrophobic core of the micelle while exposing its hydroxyl and carboxylate groups at the micelle–water interface.<sup>21,22</sup> Moreover, NaHN, being a naphthalene derivative, will also have a greater aromatic character, that is, a greater tendency to participate in noncovalent aromatic interactions ( $\pi$ – $\pi$  and cation– $\pi$ ).<sup>23–25</sup> There is a vast literature showing that the interaction of  $\pi$ -bonding systems can result in a net attractive potential.<sup>23,24</sup> Cation– $\pi$  interactions have also come to be recognized as an important class of noncovalent binding force.<sup>25</sup> In the case of planar aromatic rings, studies show that aromatic interactions are maximized when the rings are *offset-stacked* rather than stacked right on top of each other.<sup>23</sup>

We postulate that aromatic interactions are critical to the creation of aligned domains, as is shown schematically by Figure 9. When the sample is sheared, the worms will tend to align, and this will bring adjacent worms into close proximity. Since the HN counterions far outnumber the EHAC headgroups, some of the counterions will not be fully embedded in the cores of the micelles. These partially exposed HN counterions on adjacent micelles will be able to interact with each other (via offset-stacked  $\pi$ – $\pi$  interactions<sup>23</sup>) and with the adjacent cationic headgroups of the surfactant (via cation– $\pi$  interactions<sup>25</sup>). Such noncovalent interactions may be sufficient to counteract the randomizing tendency of Brownian motion and thereby stabilize aligned domains of micelles. The above mechanism suggests that aligned domains are more likely to be stabilized in the presence of NaHN rather than NaSal due to the larger  $\pi$ -bonding system of the former. This would account for our experimental results.

(21) Heindl, A.; Strand, J.; Kohler, H. H. *J. Phys. Chem.* **1993**, *97*, 742.

(22) Bijma, K.; Engberts, J. *Langmuir* **1997**, *13*, 4843.

(23) Hunter, C. A.; Lawson, K. R.; Perkins, J.; Urch, C. J. *J. Chem. Soc., Perkin Trans. 2* **2001**, 651.

(24) Waters, M. L. *Curr. Opin. Chem. Biol.* **2002**, *6*, 736.

(25) Ma, J. C.; Dougherty, D. A. *Chem. Rev.* **1997**, *97*, 1303.

(20) Gonzalez, Y. I.; Kaler, E. W. *Curr. Opin. Colloid Interface Sci.* **2005**, *10*, 256.

#### 4. Conclusions

In this study, we have described how certain wormlike micellar fluids exhibit a strong birefringence that persists for hours after cessation of shear. The birefringence is due to the samples having an arrested ("frozen") microstructure consisting of domains of aligned micelles. This effect is not a phase transition: the domains are kinetically stabilized, and the micelles do slowly revert to an isotropic state, a process that can be quickened by heating. Importantly, the aligned domains (and hence the birefringence) occur only in the presence of certain organic counterions, specifically those having a strong aromatic character, such as naphthalene derivatives. This finding suggests that the stabilization of aligned domains is facilitated by aromatic interactions ( $\pi$ - $\pi$  and cation- $\pi$ ) between counterions and headgroups from adjacent micelles.

**Acknowledgment.** We acknowledge NIST NCNR (Gaithersburg, MD) for facilitating the flow-SANS experiments performed as part of this work. We are also grateful to Dr. Dan Fry and Dr. Erik Hobbie from the Polymers Division at NIST for allowing us access to their rheo-optic experimental setup and for their assistance with the experiments. Finally, we would like to thank Zhaoliang Lin and Prof. Robert Briber (Materials Department at U. Maryland) for the use of their optical microscope.

**Supporting Information Available:** Movies corresponding to Figure 1, data from optical microscopy, and further analysis of SANS data. This material is available free of charge via the Internet at <http://pubs.acs.org>.

LA8029374

### Supporting Information for

Persistence of Birfringence in Sheared Solutions of Wormlike Micelles

Bradley D. Frounfelker, Gokul C. Kalur, Bani H. Cipriano,  
Dganit Danino and Srinivasa R. Raghavan\*

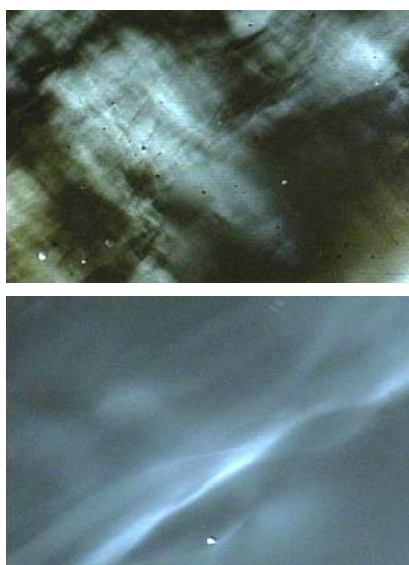


**Figure S1.** Polarized light microscopy of a 40 mM EHAC + 110 mM NaHN sample that has been subjected to shear. The residual birefringence is seen in both images. The top image corresponds to a 25X magnification, while the bottom one corresponds to 100X.

SANS patterns in the flow-vorticity plane for a 40 mM EHAC + 110 mM NaHN sample before, during, and after shear (Figure 7)

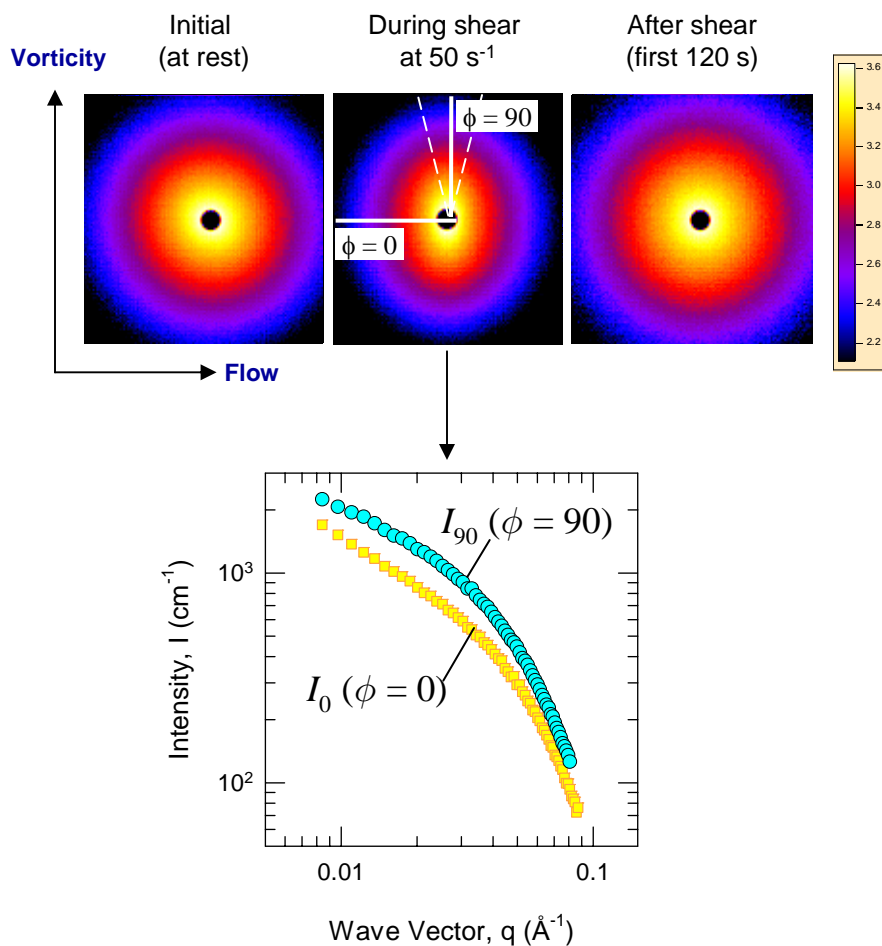


**Figure S2.** Intensity  $I$  vs. wave-vector  $q$  plots about the flow ( $I_0$ ) and vorticity ( $I_{90}$ ) directions for the anisotropic SANS pattern under shear. The data were obtained by averaging the intensity over 15° sectors centered at  $\phi = 0^\circ$  and  $90^\circ$ , as indicated on the plot (analysis similar to that in Ref. 12).